Global properties of nuclei

1. Masses, binding energies and neutron separation energies
2. Charge density distribution
3. Deformations, quadrupole moment

Binding

$$m(N,Z) = \frac{1}{c^2}E(N,Z) = NM_n + ZM_H - \frac{1}{c^2}B(N,Z)$$

- The mass of a nucleus consisting of A nucleons is not entirely determined by the masses of the nucleons. The difference (the "mass defect") is the binding energy: that energy required to disassemble the nucleus. Note that the mass is defined in terms of atomic masses (it includes the electron masses).
- The binding energy contributes significantly (~1%) to the mass of a nucleus. This implies that the constituents of two (or more) nuclei can be rearranged to yield a different and perhaps greater binding energy and thus points towards the existence of nuclear reactions in close analogy with chemical reactions amongst atoms.

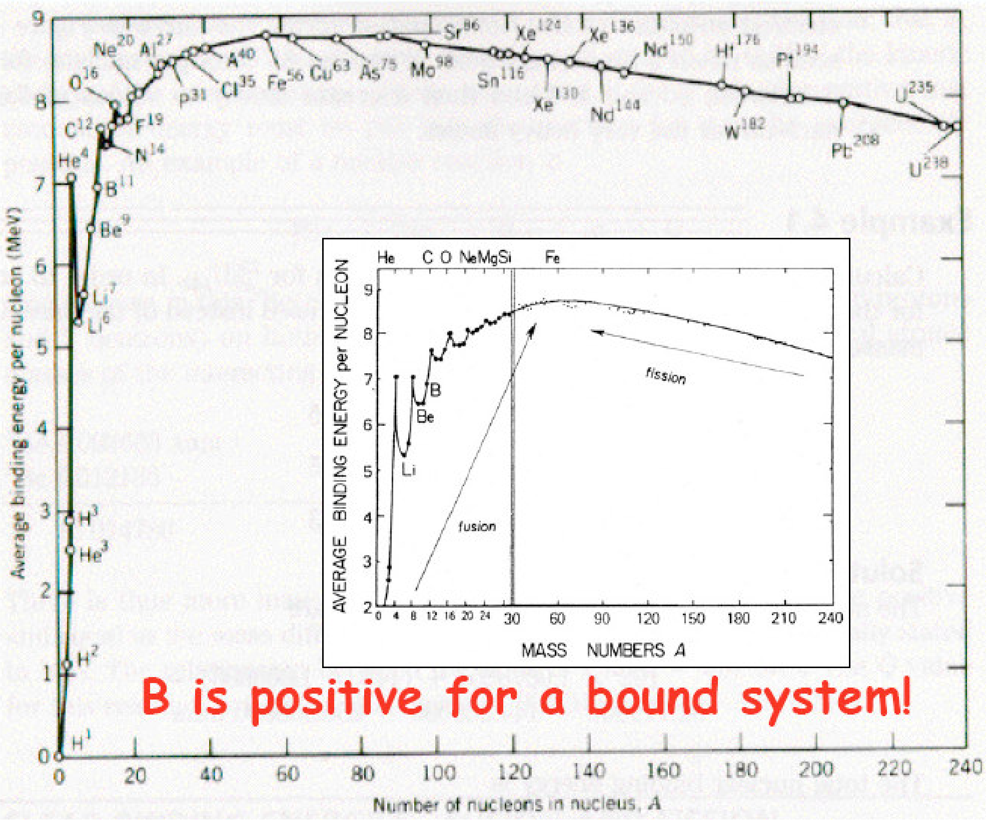

Binding: liquid-drop formula

The semi-empirical mass formula, based on the liquid drop model, considers five contributions to the binding energy(Bethe-Weizacker 1935/36)

$$B = a_{vol}A - a_{surf}A^{2/3} - a_{sym}\frac{(N-Z)^2}{A} - a_C\frac{Z^2}{A^{1/3}} - \delta(A)$$

15.68 -18.56 -28.1 -0.717

$$\delta(A) = \begin{cases} -34\,A^{-3/4} & \text{for even - even} \\ 0 & \text{for even - odd} \\ 34\,A^{-3/4} & \text{for odd - odd} \end{cases}$$

pairing term

Different contributions to binding.

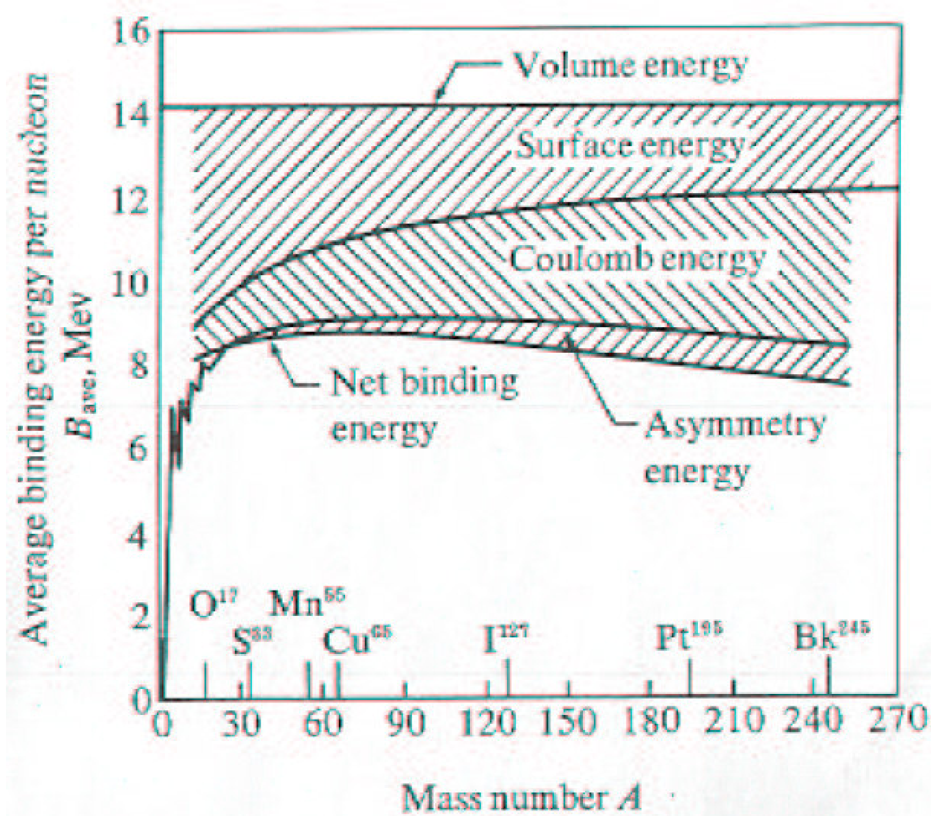

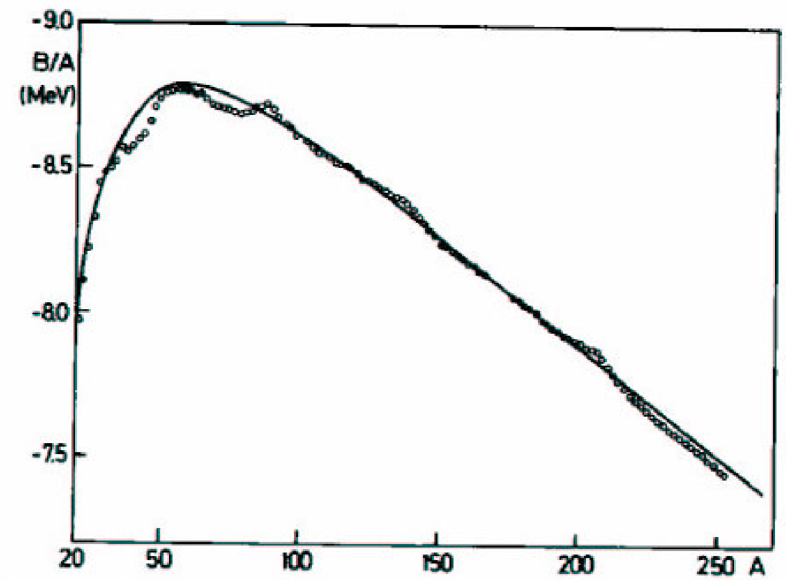

The semi-empirical mass formula, based **on the liquid drop model**, compared to the data

The liquid-drop formula reproduces the bulk properties of nuclei.

Estimates for the drip lines can be obtained from the liquid-drop model

Missing: Shell corrections and other effects from quantum mechanics.

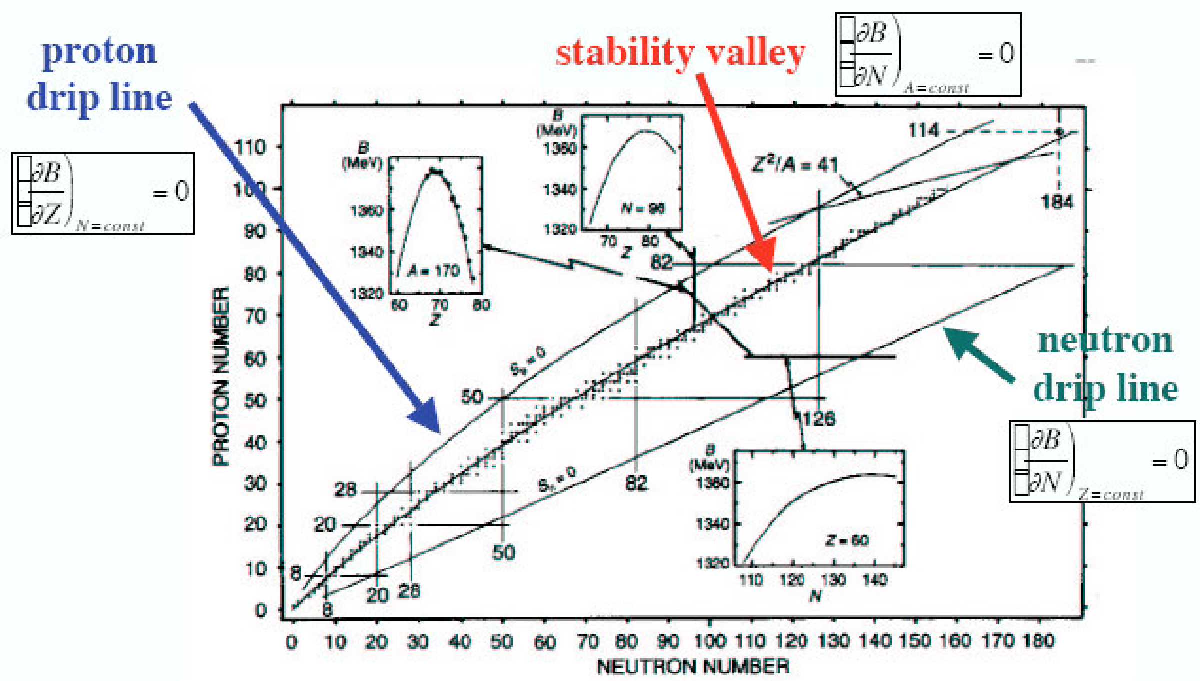

Binding energies: bulk properties

- For most nuclei, the binding energy per nucleon is about 8MeV.
- Binding is less for light nuclei (these are mostly surface) but there are peaks for A in multiples of 4. (But note that the peak for 8Be is slightly lower than that for 4He.
- The most stable nuclei are in the A~60 mass region
- Light nuclei can gain binding energy per nucleon by fusing; heavy nuclei by fissioning.
- The decrease in binding energy per nucleon for A>60 can be ascribed to the repulsion between the (charged) protons in the nucleus: the Coulomb energy grows in proportion to the number of possible pairs of protons in the nucleus Z(Z-1)/2
- The binding energy for massive nuclei (A>60) thus grows roughly as A; if the nuclear force were long range, one would expect a variation in proportion to the number of possible pairs of nucleons, i.e. as A(A-1)/2. The variation as A suggests that the force is saturated; the effect of the interaction is only felt in a neighborhood of the nucleon.

Neutron star: bold explanation

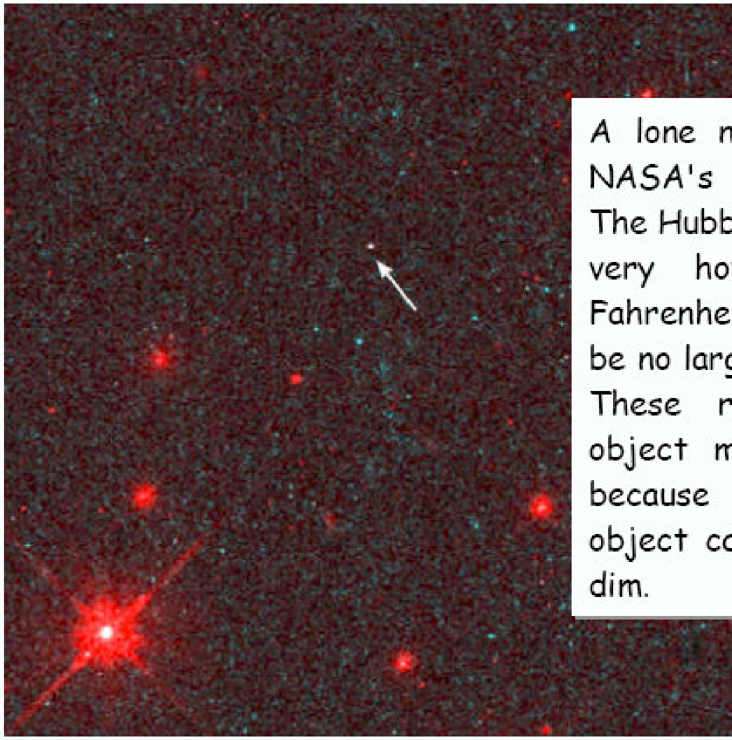

A lone neutron star, as seen by NASA's Hubble Space Telescope. The Hubble results show the star is very hot (1.2 million degrees Fahrenheit at the surface), and can be no larger than 16.8 miles across. These results prove that the object must be a neutron star, because no other known type of object can be this hot, small, and dim.

$$B = a_{vol}A - a_{surf}A^{2/3} - a_{sym}\frac{(N-Z)^2}{A} - a_C\frac{Z^2}{A^{1/3}} - \delta(A) + \frac{3}{5}\frac{G}{r_0 A^{1/3}}M^2$$

Let us consider a giant neutron-rich nucleus. We neglect Coulomb, surface, and pairing energies. Can such an object exist?

$$B = a_{vol}A - a_{sym}A + \frac{3}{5}\frac{G}{r_0 A^{1/3}}(m_n A)^2 = 0$$

limiting condition

$$\frac{3}{5}\frac{G}{r_0}m_n{}^2 A^{2/3} = 7.5\,\mathrm{MeV} \Rightarrow A \cong 5\times 10^{55}, R \cong 4.3\,\mathrm{km}, M \cong 0.045\,M_\odot$$

More precise calculations give M(min) of about 0.1 solar mass. Must neutron stars have $R \cong 10\,\mathrm{km}, M \cong 1.4\,M_\odot$

Finite-range droplet model: Möller, Nix,Myers, Swiatecki, 1994

$E(Z, N, \text{shape}) =$

$M_H Z + M_n N$	mass excess of Z hydrogen atoms and N neutrons
$+\left(-a_1 + J\bar{\delta}^2 - \frac{1}{2} K\bar{\varepsilon}^2\right)A$	volume energy
$+\left(-a_2 B_1 + \frac{9}{4} J^2 \bar{\delta}^2 B_s^2 / QB_1\right)A^{2/3}$	surface energy
$+a_3 A^{1/3} B_k$	curvature energy
$+a_0 A^0$	A^0 energy
$+c_1 \frac{Z^2}{A^{1/3}} B_3$	Coulomb energy
$-c_2 Z^2 A^{1/3} B_r$	volume redistribution energy
$-c_4 \frac{Z^{4/3}}{A^{1/3}}$	Coulomb exchange correction
$-c_5 Z^2 B_w B_s / B_1$	surface redistribution energy
$+f_0 \frac{Z^2}{A}$	proton form - factor correction to the Coulomb energy
$-c_a (N - Z)$	charge - asymmetry energy
$+W\left(\lvert I\rvert + \begin{cases} 1/A, & Z \text{ and } N \text{ odd and equal} \\ 0, & \text{otherwise} \end{cases}\right)$	Wigner energy
$+\begin{cases} +\bar{\Delta}_p + \bar{\Delta}_n - \delta_{np}, & Z \text{ and } N \text{ are odd} \\ +\bar{\Delta}_p, & Z \text{ odd and } N \text{ even} \\ +\bar{\Delta}_n, & Z \text{ even and } N \text{ odd} \\ +0, & Z \text{ and } N \text{ are even} \end{cases}$	average pairing energy
$-a_{el} Z^{2.39}$	energy of bound electrons

Shell effects

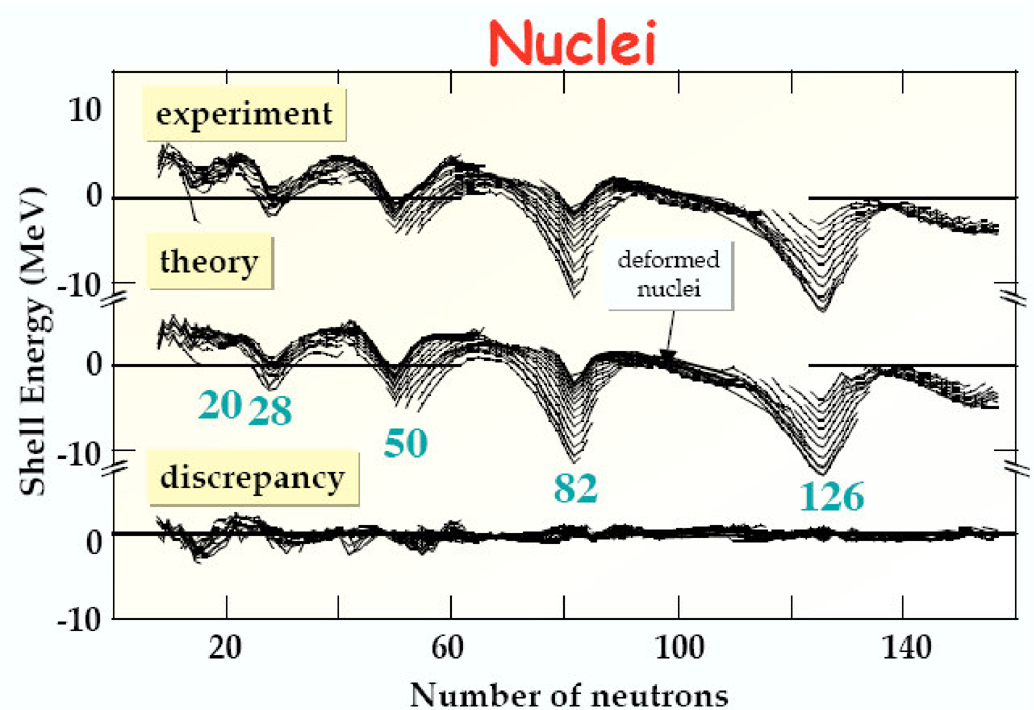

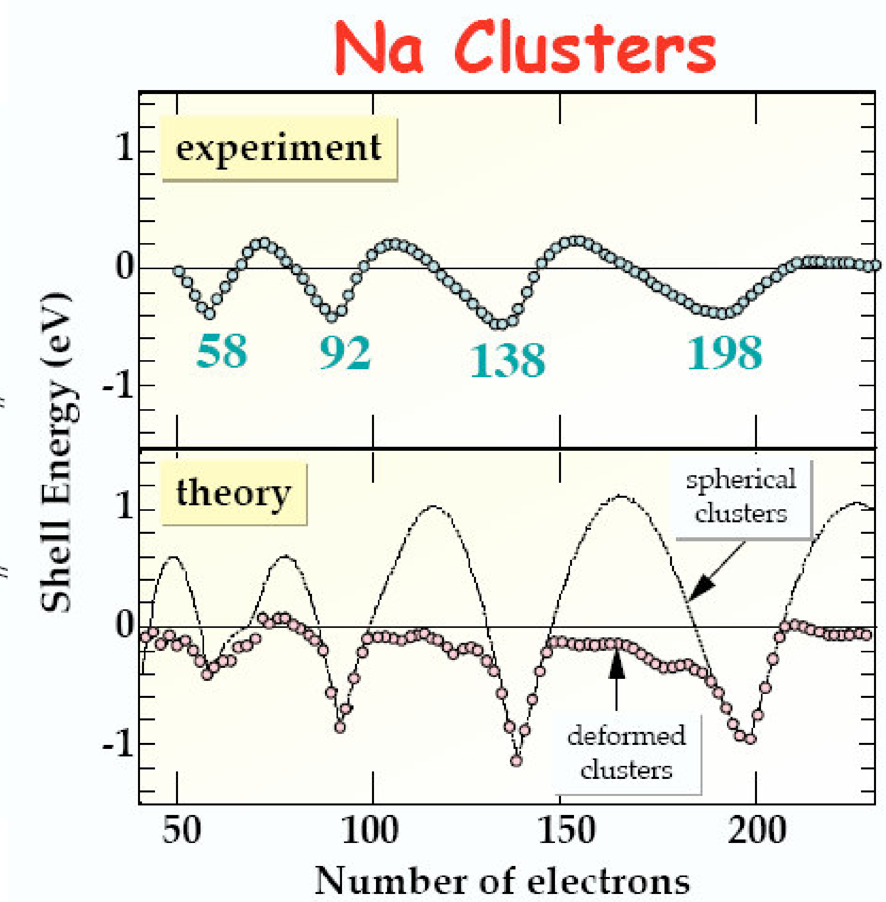

Odd-even effects

Odd-even mass difference

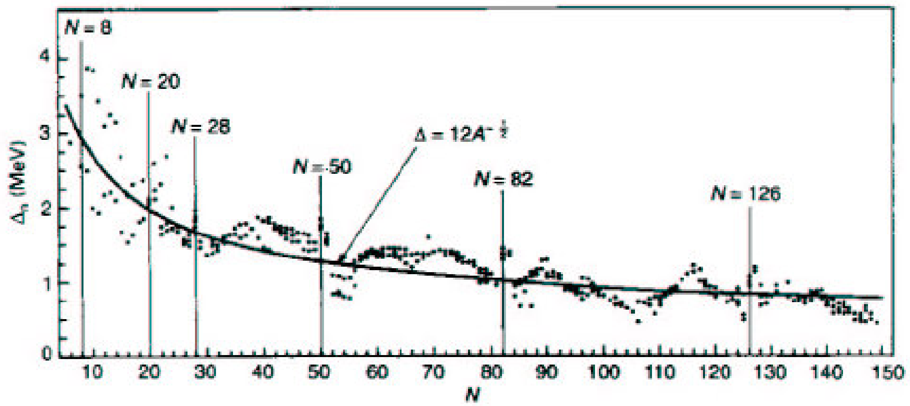

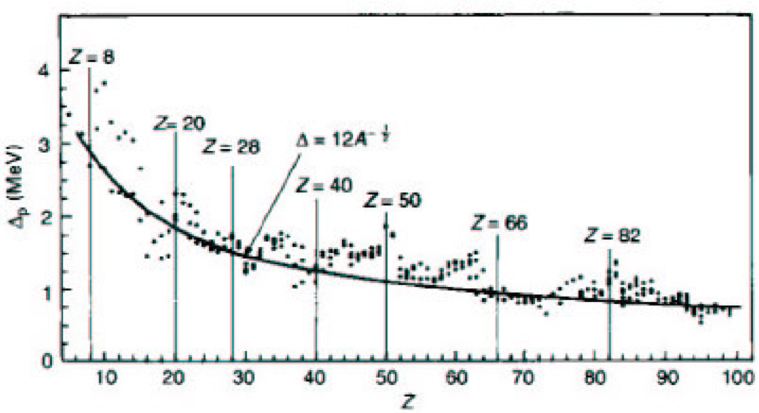

Odd-even staggering

1. Double occupancy of single-particle orbitals by spin-1/2 fermions

2. (Pairing is another component)

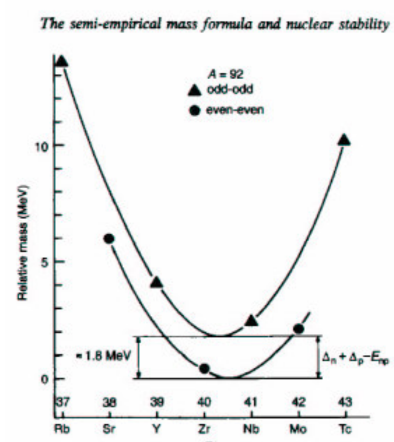

$$\Delta_n = B(N,Z) - \frac{B(N+1,Z) + B(N-1,Z)}{2}$$

$$\Delta_p = B(N,Z) - \frac{B(N,Z+1) + B(N,Z-1)}{2}$$

A common phenomenon in mesoscopic systems!

Separation Energies

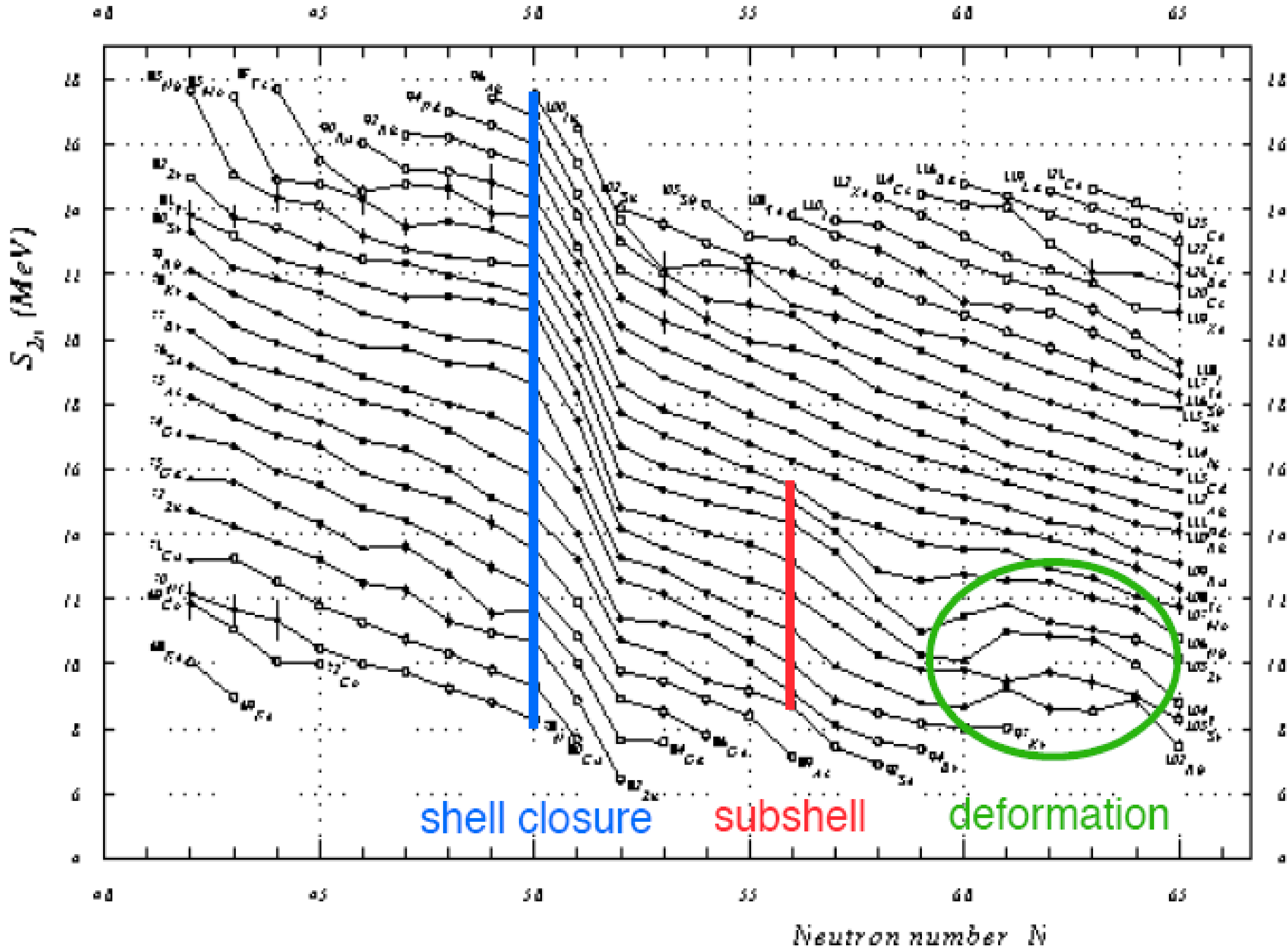

Charge-density distributions

Cross section from elastic electron scattering

$$\frac{d\sigma}{d\Omega} = \frac{d\sigma}{d\Omega}_{\text{point}} |F(q)|^2$$

Mott cross section

Form factor accounts for sub-structure

$$F(\vec{q}) = \int d^3r \rho_{ch}(\vec{r}) e^{i\vec{q}\vec{r}}$$

$$F(\vec{q}) = F(q^2) = \frac{4\pi}{q} \int_0^\infty dr r \sin qr \rho_{ch}(r)$$

Relation to geometric properties:
Expansion for small momentum transfer

$$F(q^2) \approx Z\left[1 - \frac{q^2}{6}\langle r^2 \rangle\right]$$

For a “box density”:

$$\langle r^2 \rangle = \frac{3}{5} R_{\text{geo}}$$

Size and shape

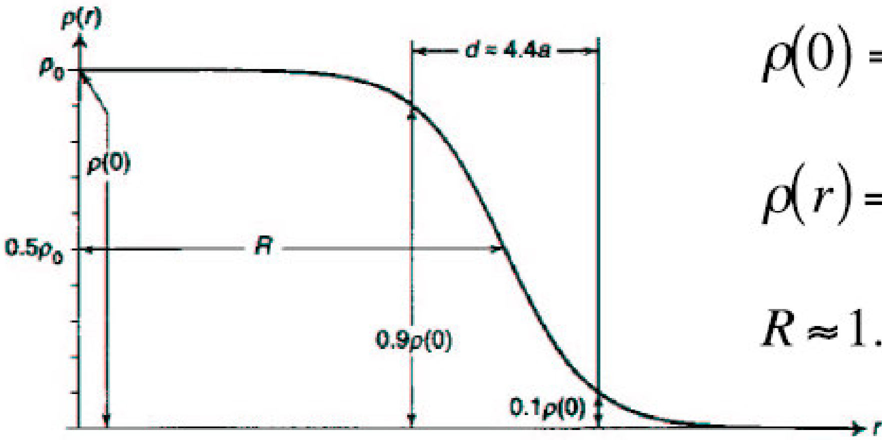

$$\rho(0) = 0.17 \text{nucleons/fm}^3$$

$$\rho(r) = \rho_0 \left[1 + \exp\left(\frac{r - R}{a}\right)\right]^{-1}$$

$$R \approx 1.2 A^{1/3} \text{fm}, \quad a \approx 0.6 \text{fm}$$

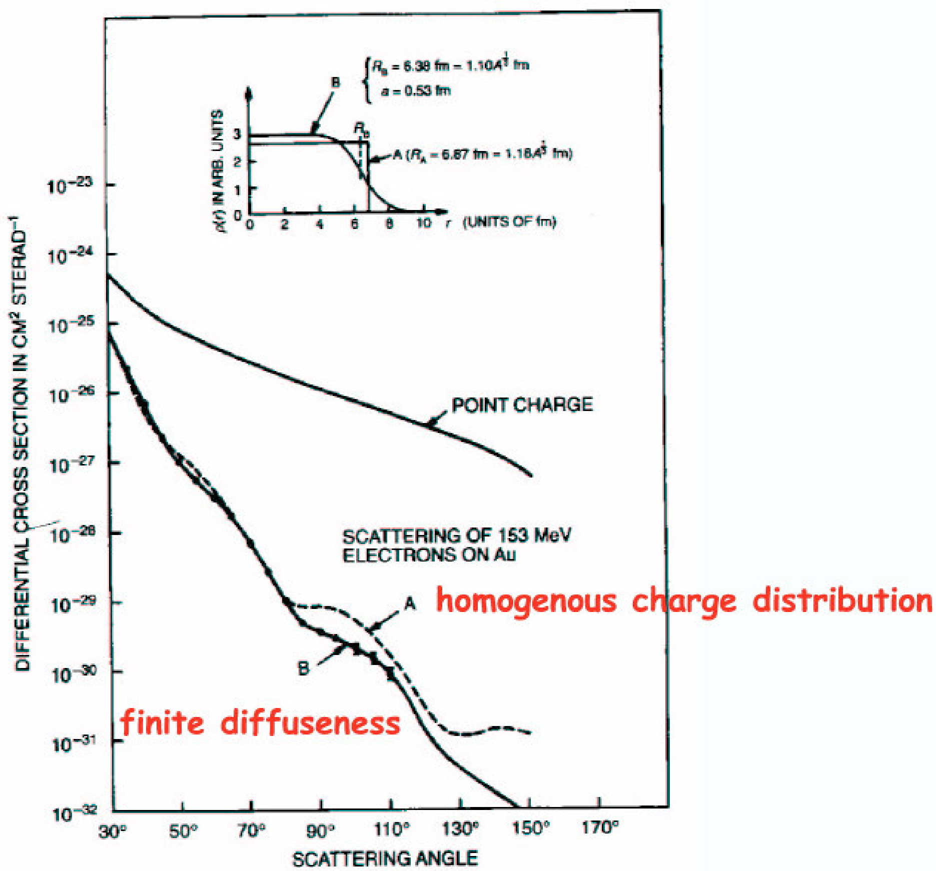

Experimental and calculated density distributions

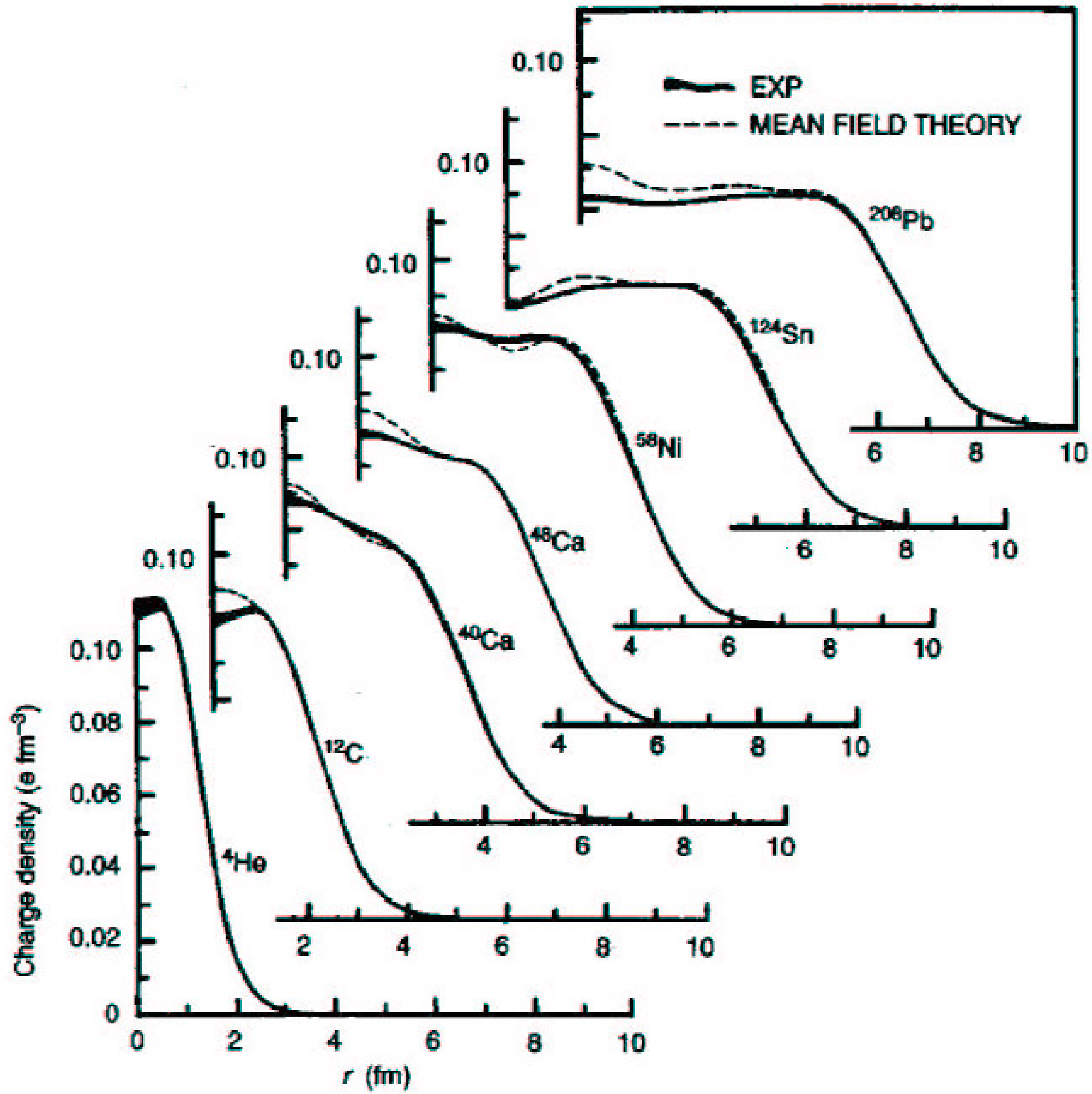

Halo nuclei

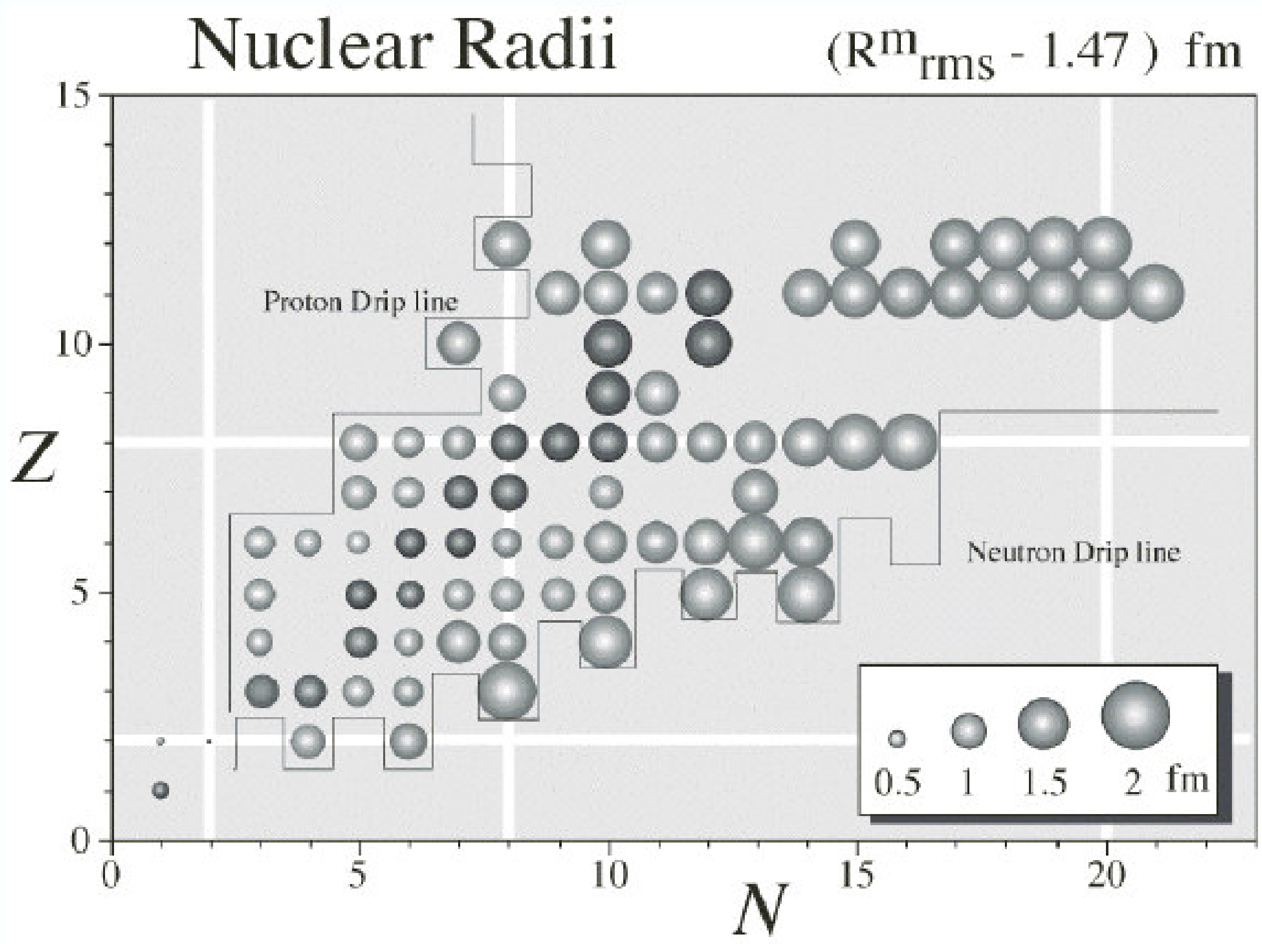

Nuclear Radii
$(R^m_{rms} - 1.47)$ fm
15
10
5
0
Z
0
5
10
15
20
N
Proton Drip line
Neutron Drip line
0.5
1
1.5
2
fm

Halo nucleus ^{11}Li

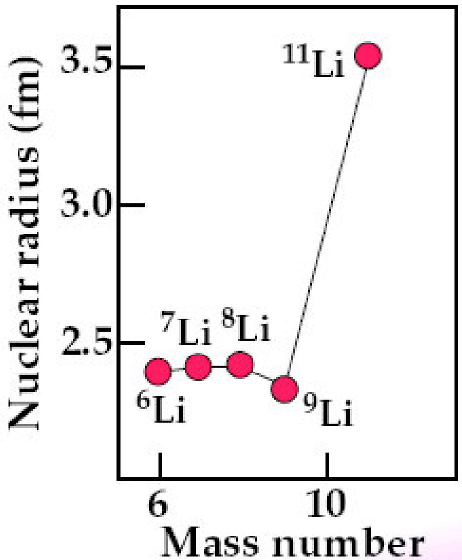

I. Tanihata et al.
Phys. Rev. Lett. 55, 2676 (1985)

Interaction cross section measurements at Bevalac (790 MeV/u)

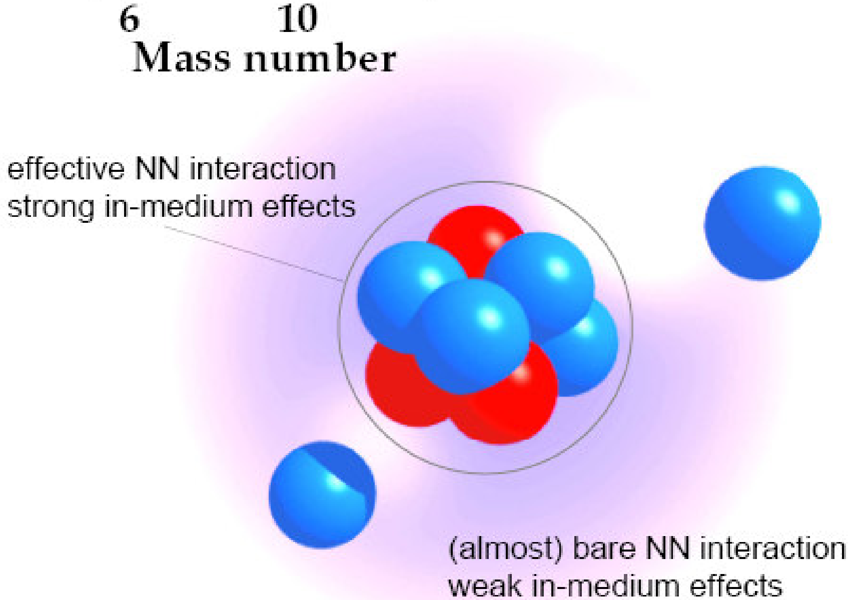

Charge radius of ^{11}Li comparable to that of ^{208}Pb !

Weakly bound system

Pairing effects essential

(^{10}Li particle-unstable nucleus)

Neutron skin vs. neutron halo

- Measure for neutron skin:

$$\delta R = \langle R_n^2 \rangle^{1/2} - \langle R_p^2 \rangle^{1/2}$$

- Neutron skins gradually build up as isotopes become more and more neutron rich.

- Halos are formed when the Fermi energy is close to the continuum, i.e. the neutron (proton) separation energy is close to zero. Due to the Coulomb barrier, proton halos are less pronounced than neutron halos. In a single-particle picture, we have

$$R_n^{\rm halo} \propto S_n^{-1/2}$$

- Neutron halos appear as one approaches the neutron drip line. They are clearly correlated to the neutron separation energy.

Halos and Fermi energy

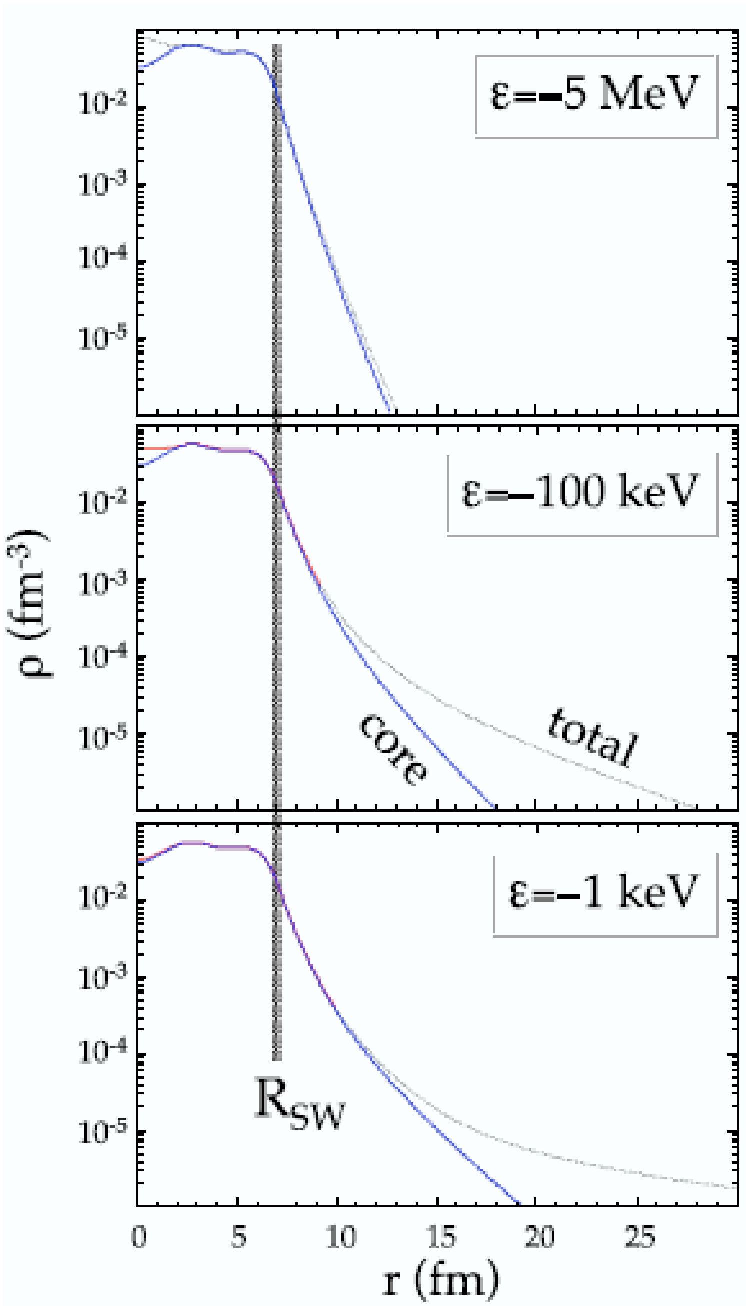

System of 70 noninteracting fermions in a square well of radius RSW and energy ϵ of the least bound orbital. The halo develops as the binding energy of the least bound orbital goes to zero.

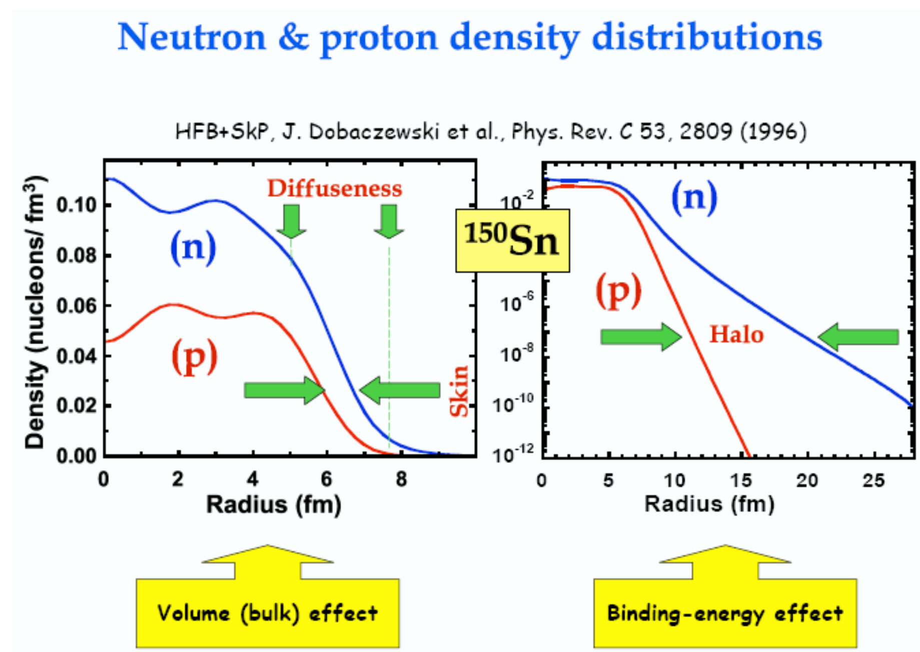

Calculated neutron skins

S. Mizutori et al., Phys. Rev. C61, 044326 (2000)

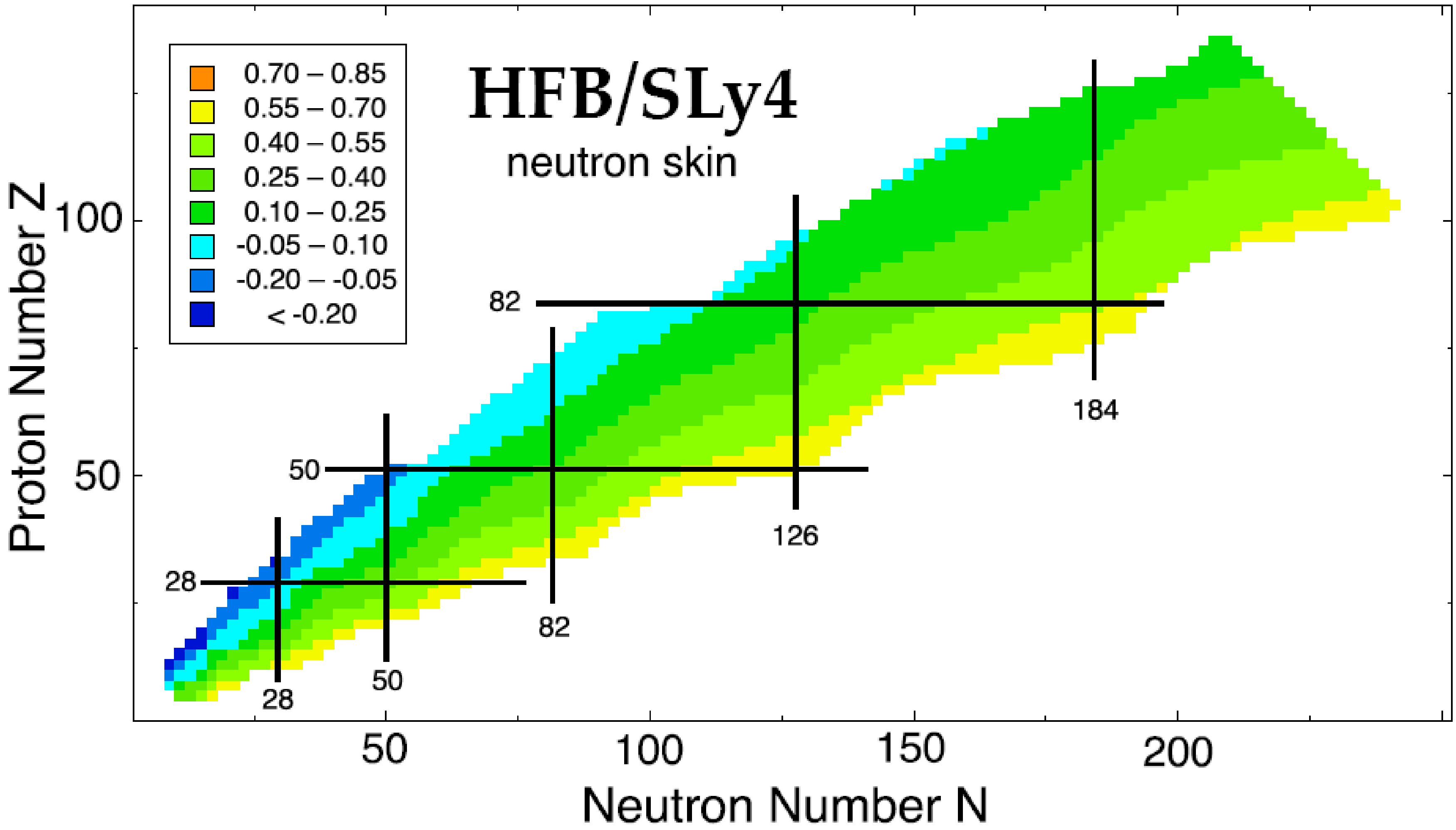

Neutron halos and separatation energies

S. Mizutori et al., Phys. Rev. C61, 044326 (2000)

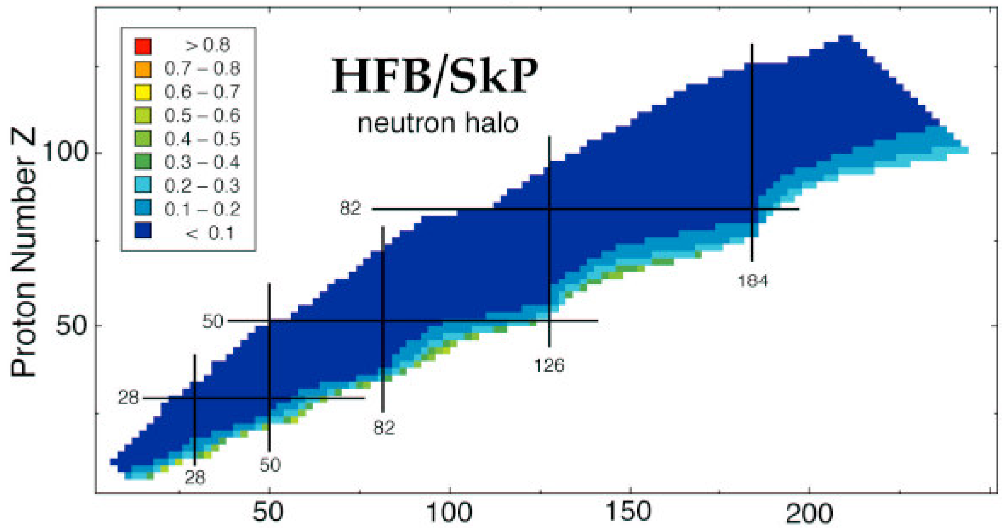

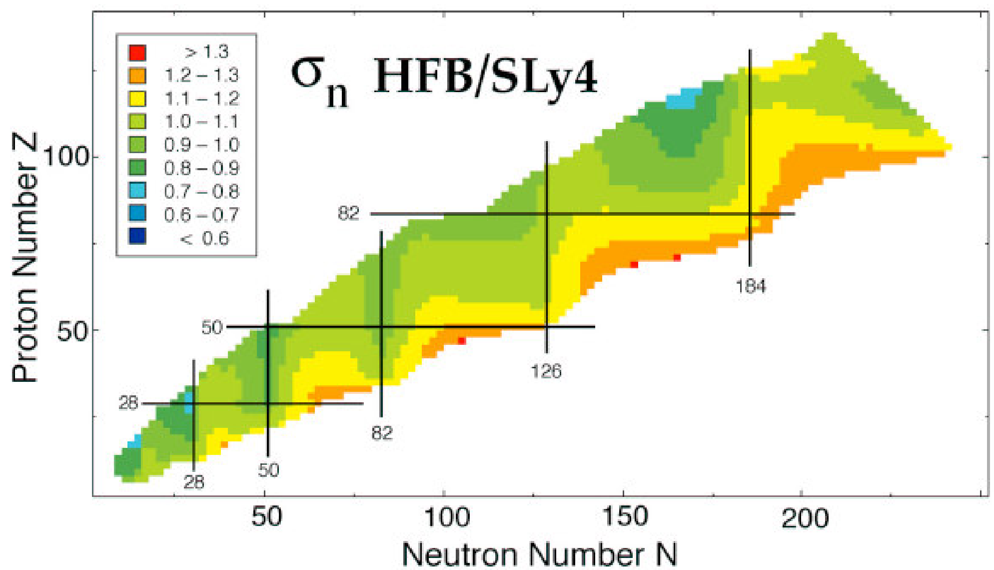

Shape deformation

The first evidence for a non-spherical nuclear shape came from the observation of a quadrupole component in the hyperfine structure of optical spectra. The analysis showed that the electric quadrupole moments of the nuclei concerned were more than an order of magnitude greater than the maximum value that could be attributed to a single proton and suggested a deformation of the nucleus as a whole.

•Schüler, H., and Schmidt, Th., Z. Physik 94, 457 (1935)
•Casimir, H. B. G., On the Interaction Between Atomic Nuclei and Electrons, Prize Essay, Taylor's Tweede Genootschap, Haarlem (1936)

The question of whether nuclei can rotate became an issue already in the very early days of nuclear spectroscopy

•Thibaud, J., Comptes rendus 191, 656 (1930)
•Teller, E., and Wheeler, J. A., Phys. Rev. 53, 778 (1938)
•Bohr, N., Nature 137, 344 (1936)
•Bohr, N., and Kalckar, F., Mat. Fys. Medd. Dan. Vid. Selsk. 14, no, 10 (1937)

Static electric quadrupole moment

Hyperfine atomic splitting (of order 10^{-7} eV) due to quadrupole deformation of nucleus. Electric potential

$$\phi(\vec{r}) = \left[\frac{1}{4\pi\varepsilon_0}\right]\int d^3r' \frac{\rho(\vec{r}')}{|\vec{r}-\vec{r}'|}.$$

Multipole expansion valid if charge distribution is probed at large distances $|\vec{r}| \gg |\vec{r}'|$:

$$\phi(\vec{r}) = \left[\frac{1}{4\pi\varepsilon_0}\right]\sum_{\lambda=0}^{\infty}\sum_{\mu=-\lambda}^{\lambda}\frac{4\pi}{(2\lambda+1)r^{\lambda+1}}Y_{\lambda\mu}(\theta,\varphi)Q_{\lambda\mu},$$

with multipole moments

$$Q_{\lambda\mu} = \int d^3r'(r')^{\lambda}Y_{\lambda\mu}(\theta',\varphi')\rho(\vec{r}').$$

All moments $Q_{\lambda\mu}$ with odd λ vanish. $Q_{00} = Z$, and the first nontrivial moment is quadrupole moment $Q_{2\mu}$.

For axially symmetric charge distributions,

$$Q_{20} = \sqrt{\frac{5}{16\pi}}\int d^3r'(r')^2(3\cos^2\theta'-1)\rho(\vec{r}') = \sqrt{\frac{5}{16\pi}}\int d^3r'(3z'^2-r'^2)\rho(\vec{r}')$$

fully determines the quadrupole moment: In the body-fixed frame one has $Q_{20} = Q_{z'z'} = -2Q_{x'x'} = -2Q_{y'y'}$. Note that $Q_{20} > 0$ for prolate (cigar shaped) charge distributions and $Q_{20} < 0$ for oblate (discus like) charge distributions.

Shape deformations

Shape deformations

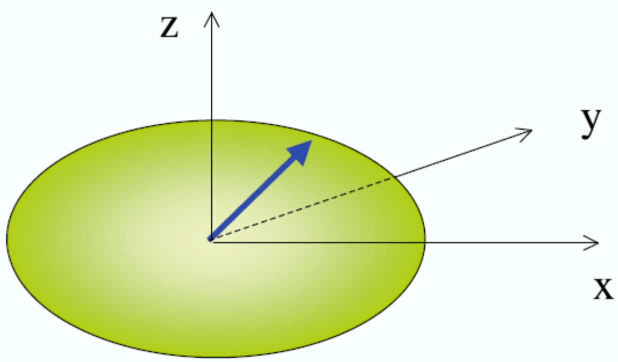

$$R(\theta,\varphi) = c(\alpha) R_0 \left[1 + \sum_{\lambda=1} \sum_{\mu=-\lambda}^{\lambda} \alpha^*_{\lambda\mu} Y_{\lambda\mu}(\theta,\varphi) \right]$$

volume conservation

radius of the sphere
with the same volume

deformation parameters
For axial shapes $\mu=0$

$$\beta_\lambda \equiv \alpha_{\lambda\mu}$$

a) $\lambda=1$ (dipole); $\mu=-1,0,1$

$$\underbrace{\int_V \vec{r} d^3 r = 0}_{}$$ center of mass conservation

3 conditions, they fix $\alpha_{1\mu}$

b) $\lambda=2$ (quadrupole); $\mu=-2,-1,0,1,2$

$$\underbrace{\alpha_{21} = \alpha_{2-1} = 0, \quad \alpha_{22} = \alpha_{2-2}}$$

3 conditions, they fix three Euler angles

Only two deformation parameters left:C

$$\alpha_{20} = \beta \cos\gamma, \quad \alpha_{22} = \frac{1}{\sqrt{2}} \beta \sin\gamma$$

(β,γ are the so-called Hill- Wheeler coordinates)

c) $\lambda=3$ (octupole)
d) $\lambda=4$ (hexadecupole)
e) …

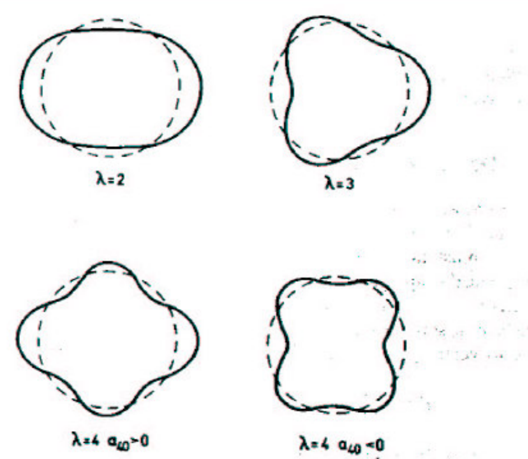

Quadrupole moments and electric E2 transitions

Strength for electric quadrupole transitions

$$B(E2) \propto Q_{20}^2$$

Across the table of nuclides one finds the following trends for transitions from a 0^+ ground state to a 2^+ excited state:

1. $B(E2)$ increase with mass
2. $B(E2)$ are particularly small around closed shells as closed shell nuclei have spherical ground states and deformations are energetically expensive.

Shell structure: B(E2) and E_2^+

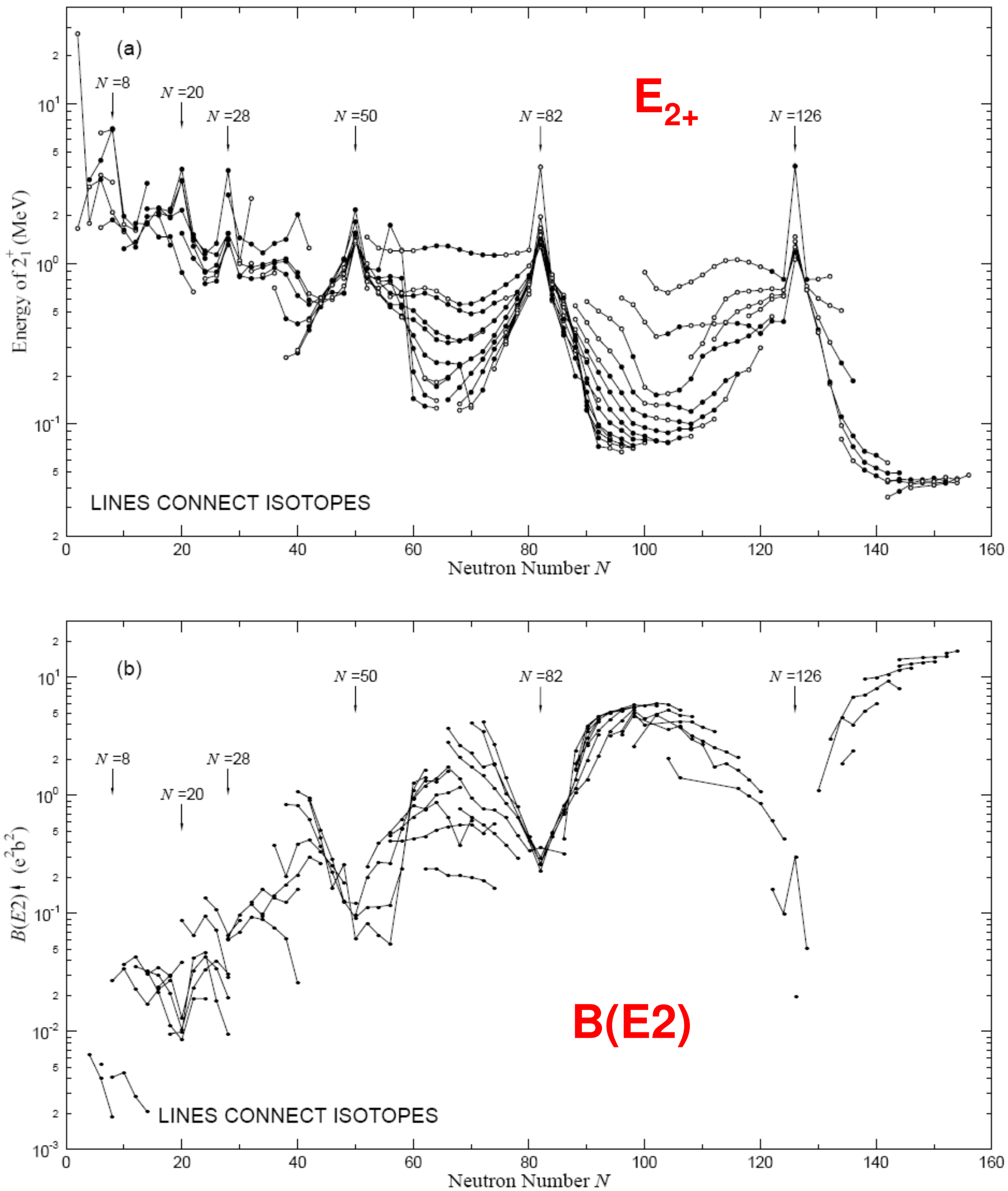

Nuclei with magic N

- Relatively high-lying first 2^+ exited state
- Relatively low B(E2) transition strength

S. Raman et al, Atomic Data and Nuclear Data Tables 78 (2001) 1.